



## Therapeutic Effect of AAV8-Mediated miR-23a in Immobilization-Induced Muscle Atrophy in Mice

Lu Na<sup>1,2</sup>, Wang Yijin Zhang<sup>3</sup>, Wenxin<sup>1</sup>, Farra Aidah Jumuddin<sup>2\*</sup>

<sup>1</sup>Hainan Medical University, Hainan, 570102, China

<sup>2</sup>Lincoln University College, Wisma Lincoln, 12-18, Jalan SS 6/12, 47301 Petaling Jaya, Selangor, Malaysia

<sup>3</sup>Emergency and Trauma College of Hainan Medical University, Hainan, 570102, China

\*Correspondence E-mail: [farraaidah@lincoln.edu.my](mailto:farraaidah@lincoln.edu.my)

### Abstract

Objective: To investigate the therapeutic effect of miR-23a in immobilization-induced muscle atrophy in mice. Methods: (Experiment 1) Twelve C57BL6 wild-type mice were randomly divided into two groups: Sham group (sham surgery) and Immobilization (hind limb immobilization surgery). Fluorescence quantitative PCR was performed to detect the expression changes of miR-23a, MuRF-1, and Atrogin-1 7 days post-surgery. (Experiment 2) Twelve C57BL6 wild-type mice were randomly divided into 4 groups according to surgery type (sham surgery and hind limb immobilization surgery) and injection type (AAV8 or AAV8-OEmiR-23a), fluorescence quantitative PCR to detect changes in MuRF-1 and Atrogin-1 expression in mouse gastrocnemius muscle. (Experiment 3) NFATc3 expression changes were detected by fluorescence quantitative PCR 48 hours post-transfection. (Experiment 4) Twelve C57BL6 wild-type mice underwent hind limb immobilization surgery, divided into 4 groups: Immobilization+AAV8-control, Immobilization+AAV8-OEmiR23a, Immobilization+AAV8-shNFATc3, and Immobilization+AAV8-OEmiR-23a+AAV8-shNFATc3. quantitative PCR to detect changes in MuRF-1 and Atrogin-1 expression in mouse gastrocnemius muscle. Results: Fluorescence quantitative PCR results showed that miR-23a was downregulated in immobilization-induced muscle atrophy, while MuRF-1 and Atrogin-1 expression was upregulated. WGA staining results showed that intramuscular injection of AAV8-OEmiR-23a could significantly alleviate the decrease in muscle fiber cross-sectional area and the increase in expression of muscle atrophy marker genes MuRF-1 and Atrogin-1 caused by hind limb immobilization. Fluorescence quantitative PCR revealed that when miR-23a expression was inhibited, NFATc3 expression was downregulated; when miR-23a was overexpressed, NFATc3 expression was upregulated. Fluorescence quantitative PCR results showed that intramuscular injection of AAV8-OEmiR-23a and AAV8-shNFATc3 could not alleviate the increase in expression of muscle atrophy marker genes MuRF-1 and Atrogin-1 caused by hind limb immobilization. Conclusion: miR-23a can treat hind limb immobilization-induced muscle atrophy in mice.

**Keywords:** miR-23a, hind limb immobilization-induced muscle atrophy, NFATc3

### Introduction

The occurrence of muscle atrophy is attributed to increased muscle fatigue, decreased muscle fibers, reduced muscle protein synthesis, and increased ubiquitination degradation (Ryu *et al.*, 2019). For example, ubiquitination-related proteins MuRF-1 and Atrogin-1 show significantly elevated expression levels during the process of muscle atrophy. Various metabolic abnormalities in the body can lead to

muscle atrophy, including fasting, cancer, sepsis, diabetes, and reduced mechanical loads (Wang *et al.*, 2024). However, not all types of muscle fibers exhibit muscle atrophy. Skeletal muscles composed of different fiber types have distinct contraction and metabolic characteristics. Slow-twitch fibers typically contain abundant mitochondria and capillaries, while fast-twitch fibers do not. Hind limb suspension is a commonly used animal model to reduce mechanical loads, simulating prolonged spaceflight. During this process, slow-twitch muscles often exhibit more pronounced atrophy than fast-twitch muscles (Ismaeel *et al.*, 2023; Petrocelli *et al.*, 2024). However, there are also exceptions, as hind limb immobilization induces similar muscle atrophy with a decrease in muscle mass percentage in both slow and fast muscles (Reidy *et al.*, 2023; Takahashi *et al.*, 2023). A method that significantly induces muscle atrophy in the hind limb muscles of mice is casting fixation. Implementing a casting fixation model in mice presents unique technical challenges due to their small size. Clinical data from studies on bed rest in humans also indicate a significant decrease in the cross-sectional area of fast-twitch fibers in the lateral thigh due to casting fixation, simulating clinical muscle atrophy effects effectively (Kutz *et al.*, 2023).

Non-coding RNAs, known as microRNAs (miRNAs), play important roles in various biological and pathological processes including skeletal muscle differentiation and morphogenesis (Horak *et al.*, 2016). miRNAs are approximately 22 nucleotides in length and regulate the translation of specific mRNA targets by interacting with the 3' untranslated region (3'UTR) of targets (Altana *et al.*, 2015).

In skeletal muscle, some muscle-specific miRNAs have been reported to play various roles in controlling muscle growth and differentiation. Muscle-specific miR-1 and miR-133 regulate muscle differentiation by down regulating serum response factor and histone deacetylase 4. It has also been shown that the myogenic regulatory factor MyoD can induce miR-206 to promote myogenesis (Dong *et al.*, 2019; Ikenaka *et al.*, 2023). These previous studies have revealed the importance of muscle-specific miRNAs in skeletal muscle development. However, the role of miRNAs in adult skeletal muscle plasticity has not been reported (Koutalianos *et al.*, 2015). In this study, we found that over expression of miR-23a can treat hind limb immobilization-induced muscle atrophy in mice, providing a promising therapeutic direction for the treatment of muscle atrophy caused by prolonged bed rest in humans.

## Materials and Methods

### Materials

1. Experimental Materials: Mature muscle tube cells; C57BL6 mice

1) Mature muscle tube cells were differentiated from myoblasts C2C12, purchased from the Shanghai Institute of Biological Sciences. Specific culture and differentiation conditions are described in Methodology 2).

2) C57BL6 mice were purchased from Nanjing Model Biological Co., Ltd. They were bred in SPF-grade animal facilities. Experimental procedures involving mice have been approved by the Animal Experiment License and Animal Ethics Review Certificate.

2. Main Reagents and Instruments: RNA reverse transcription kit (Thermo Fisher); Trizol (TAKARA); TB Green (TAKARA); miR-23a primer (RiboBio); MuRF primer (Huada Gene); Atrogin-1 primer (Huada Gene); OE-miR-23a plasmid (JieRui Bio); WGA powder (Sigma); miR-23a mimic (RiboBio); miR-23a inhibitor (RiboBio); Lipofectamine® 2000 (Sigma); horse serum (BI); fetal bovine serum (BI); dual antibodies (BI); DMEM culture medium (Corning); fixation bone needles (Sangon Biotech); surgical instruments (Sangon Biotech).

### Methods

1) Hind Limb Immobilization Surgery: Mice were anesthetized with isoflurane 30 minutes before the immobilization surgery. After anesthesia, they were placed on the surgical table, and leg hair was gently removed. The foot was fixed using an automatic skin stapler, with the tibia in a normal flexed position. One bone needle was fixed near the metatarsals, and another was fixed at the distal end of

the gastrocnemius muscle. The other hind limb served as a control. After 7 days of surgical immobilization, the bone needles were removed, and AAV8 virus was injected into the mouse muscles in situ.

2) Culturing Mature Muscle Tube Cells: C2C12 cell growth culture medium contained 10% fetal bovine serum and 100 µg/ml antibiotics. When the cell growth density reached about 60%, differentiation was initiated. Differentiation medium, consisting of DMEM culture medium containing 5% horse serum and antibiotics, was used instead of the growth medium. The differentiation process lasted for 5 days and was carried out at 37°C in a cell culture incubator containing 5% CO<sub>2</sub>, until mature muscle tube cells appeared.

3) Fluorescence Quantitative PCR (qPCR): Total RNA was extracted from frozen gastrocnemius muscle and C2C12 muscle tubes using Trizol. Following the instructions of the RNA reverse transcription kit, RNA was reverse transcribed using reverse transcriptase II. qPCR was performed using 50 ng of template cDNA. The reaction conditions were as follows: initial denaturation at 95°C for 5 min, followed by 40 cycles of denaturation at 95°C, annealing at 56°C, and extension at 72°C for 40 s each. qPCR detection was performed using the Rotor-Gene 6000 (Corbett Robotics, Australia) and iQSYBR Green Supermix (BioRad). The results were analyzed using the 2- $\Delta\Delta$ Ct method for relative quantification. Primer sequences are shown in Table 1. 18s were used as internal controls.

**Table 1:** Primer sequences for qPCR

Gene	Primer sequence (5'-3')
MuRF-1	Forward: 5'- GTGTGAGGTGCCTACTTGCTC -3'
	Reverse: 5'- GCTCAGTCTTCTGTCCCTTGA -3'
Atrogin-1	Forward: 5'- CAGCTTCGTGAGCGACCTC -3'
	Reverse: 5'- GGCAGTCGAGAAGTCCAGTC -3'
18s	Forward: 5'- TCAAGAACGAAAGTCGGAGG -3'
	Reverse: 5'- GGACATCTAAGGGCATCAC -3'
NFATc3	Forward: 5'- TCGGAGTTACGGCTAGACT -3'
	Reverse: 5'- CATTGTCGACCGTTCCAA-3'

4) WGA Staining: Frozen sections were fixed with 4% paraformaldehyde at room temperature for 20 minutes, followed by staining with WGA dye at room temperature in the dark for 20 minutes according to the instructions. After rinsing with PBS, the sections were mounted with glycerol.

5) Transfection of miR-23a mimic and miR-23a inhibitor into cells: Muscle tube cells were starved for 12 hours before transfection. Lipofectamine® 2000 transfection reagent was used to transfect miR-23a mimic and miR-23a inhibitor at a concentration of 100 µM. After transfection for 12 hours, fresh culture medium was replaced, and the cells were cultured at 37°C in a CO<sub>2</sub> incubator for 48 hours.

6) AAV8 Virus Packaging: AAV8, Helper, and shuttle vector plasmids were added in equal proportions to a culture dish. PEI was added at 9 times the volume, and the total volume was adjusted to 1 mL with culture medium. After thorough mixing, the mixture was allowed to stand at room temperature for 15 minutes. Then, 1 mL of the above mixture was added to each dish of cells. After 9-10 hours, the medium was changed, and fresh complete culture medium was added. After transfection for 60 hours, the cell culture supernatant was collected into centrifuge tubes and centrifuged at 4000 rpm, 4°C for 20 minutes. The concentrated supernatant was used for animal injection.

7) In situ Injection of AAV8-OEmiR23a into Mouse Muscles: The leg hair of the mouse was removed to expose the gastrocnemius muscle. AAV8 virus, purified and concentrated, was injected into the muscle at two points, at a dose of 108 TU per mouse. The control group was injected with AAV8-control. After virus injection, the mice were returned to the animal facility and housed for 3 weeks.

8) Statistical Analysis: Statistical analysis of the data was performed using SPSS 20.0 software. Data are presented as the mean ± standard deviation (SD). One-way analysis of variance and independent samples t-test were used to determine the statistical significance between groups. A p-value less than 0.05 was considered statistically significant.

## Results

### Downregulation of miR-23a in the mouse hind limb immobilization-induced muscle atrophy model

Muscle samples were taken from the gastrocnemius muscle of mice that underwent hind limb immobilization surgery. Total RNA was extracted, reverse transcribed into cDNA, and fluorescence quantitative PCR was performed to detect the expression of MuRF-1, Atrogin-1, and miR-23a. Additionally, the leg circumference of the immobilized leg was measured. The results showed that the expression of MuRF-1 and Atrogin-1 was significantly upregulated in the gastrocnemius muscle of mice that underwent immobilization surgery (Figure 1A), and the leg circumference was significantly reduced (Table 1), indicating the successful establishment of a mouse model of muscle atrophy induced by hind limb immobilization. Furthermore, miR-23a was downregulated in the mouse hind limb immobilization-induced muscle atrophy model (Figure 1B).

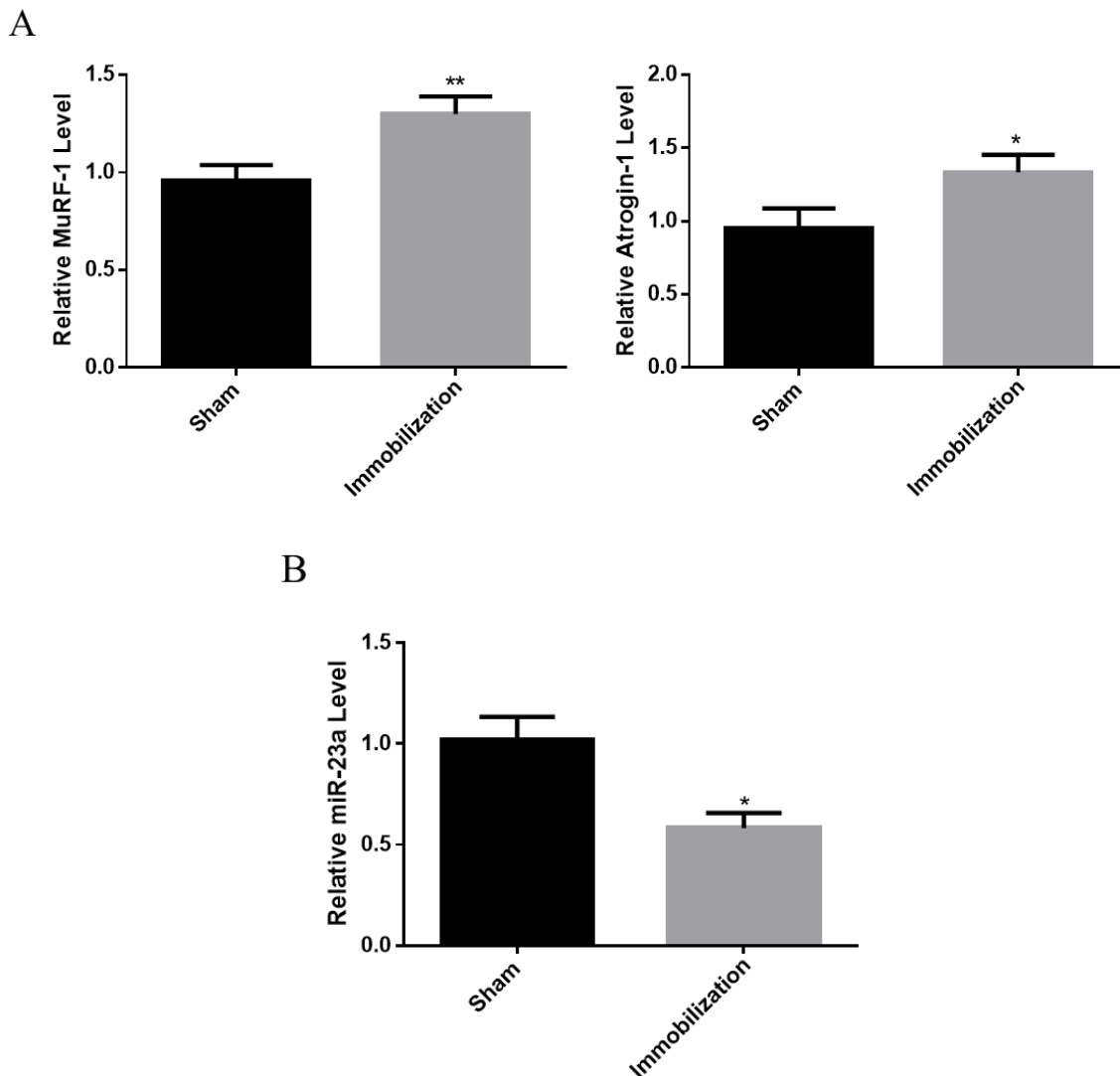


**Figure 1:** Expression Changes of miR-23a in the Gastrocnemius Muscle of Mice after Hind Limb Immobilization Surgery. A: Changes in the expression of MuRF-1 and Atrogin-1 in the gastrocnemius muscle of mice in the Immobilization group compared to the Sham group, \*,  $P < 0.05$ , \*\*,  $P < 0.01$ ,  $n = 6$ ; Table 1: Comparison of leg circumference between hind limb immobilized mice and sham surgery mice; B: Changes in miR-23a expression in the gastrocnemius muscle of mice in the Immobilization group compared to the Sham group, \*,  $P < 0.05$ ,  $n = 6$ .

**Table2:** Comparison of Leg Circumference between Hind Limb Immobilized and Sham Surgery Mice

Group	Total Number (n)	Average Leg Circumference (cm)	Atrophy Positive Rate	Significance
Hind Limb Immobilized	6	1.0±0.03	100%	P<0.05
Sham Surgery	6	1.5±0.04	0	

### *In situ* Injection of AAV8-OEmiR23a into Mouse Gastrocnemius Muscle Alleviates Immobilization-induced Muscle Atrophy

After establishing the mouse model of muscle atrophy induced by hind limb immobilization, rescue treatment experiments were conducted by injecting AAV8-OEmiR23a into the muscle *in situ*. Frozen sections of the gastrocnemius muscle were prepared from experimental mice. WGA staining results showed that *in situ* injection of AAV8-OEmiR23a into the muscle significantly alleviated the reduction in cross-sectional area of the gastrocnemius muscle caused by hind limb immobilization (Figure 2A). The expression levels of the muscle atrophy marker genes MuRF-1 and Atrogin-1 were also significantly reduced (Figure 2B). This indicates that miR-23a can to some extent treat muscle atrophy induced by hind limb immobilization.

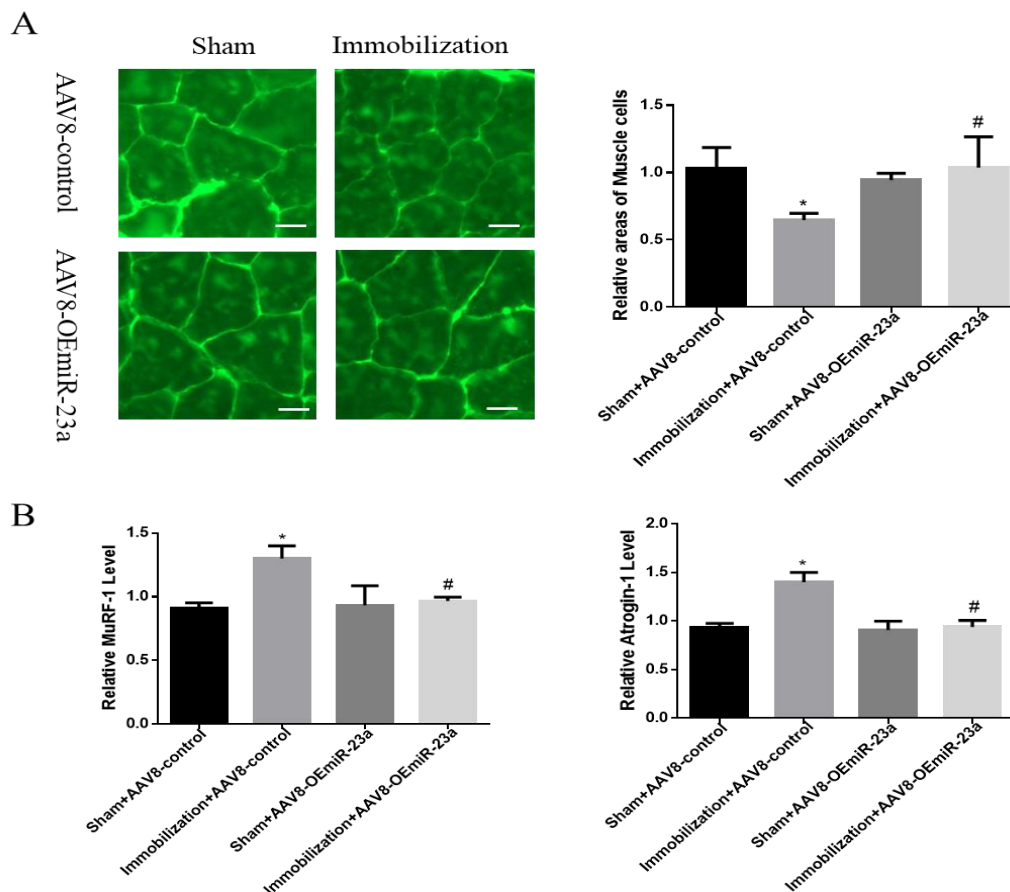


**Figure 2:** AAV8-OEmiR23a Alleviates Immobilization-induced Muscle Atrophy. A: *In situ* injection of AAV8-OEmiR23a into the mouse gastrocnemius muscle after hind limb immobilization surgery. WGA staining was performed to detect changes in muscle fiber cross-sectional area, \*,  $P < 0.05$ ,  $n = 3$ ; B: Fluorescence quantitative PCR was used to detect changes in the expression of MuRF-1 and Atrogin-1 in the mouse gastrocnemius muscle, \*, #,  $P < 0.05$ ,  $n = 3$ . Scale: 100  $\mu\text{m}$ . \*: immobilization + AAV8-control vs sham + AAV8-control; #: immobilization + AAV8-OEmiR23a vs immobilization + AAV8-control.

*Interaction between miR-23a and NFATc3 Regulates Muscle Atrophy Process*

After transfection of miR-23a mimic into mature muscle tube cells, the expression level of NFATc3 decreased (Figure 3A); after transfection of miR-23a inhibitor, the expression level of NFATc3 increased (Figure 3B), indicating the interaction between miR-23a and NFATc3. After establishing the mouse model of muscle atrophy induced by hind limb immobilization, in situ injection of AAV8-OEmiR23a and AAV8-OE NFATc3 into the muscle was performed to detect whether miR-23a and NFATc3 interacted to jointly regulate the process of muscle atrophy. The results of fluorescence quantitative PCR showed that in situ injection of AAV8-OEmiR23a and AAV8-OE NFATc3 into the muscle did not alleviate the increase in expression levels of the muscle atrophy marker genes MuRF-1 and Atrogin-1 caused by hind limb immobilization in mice. This indicates that miR-23a and NFATc3 interact to jointly regulate the process of muscle atrophy.

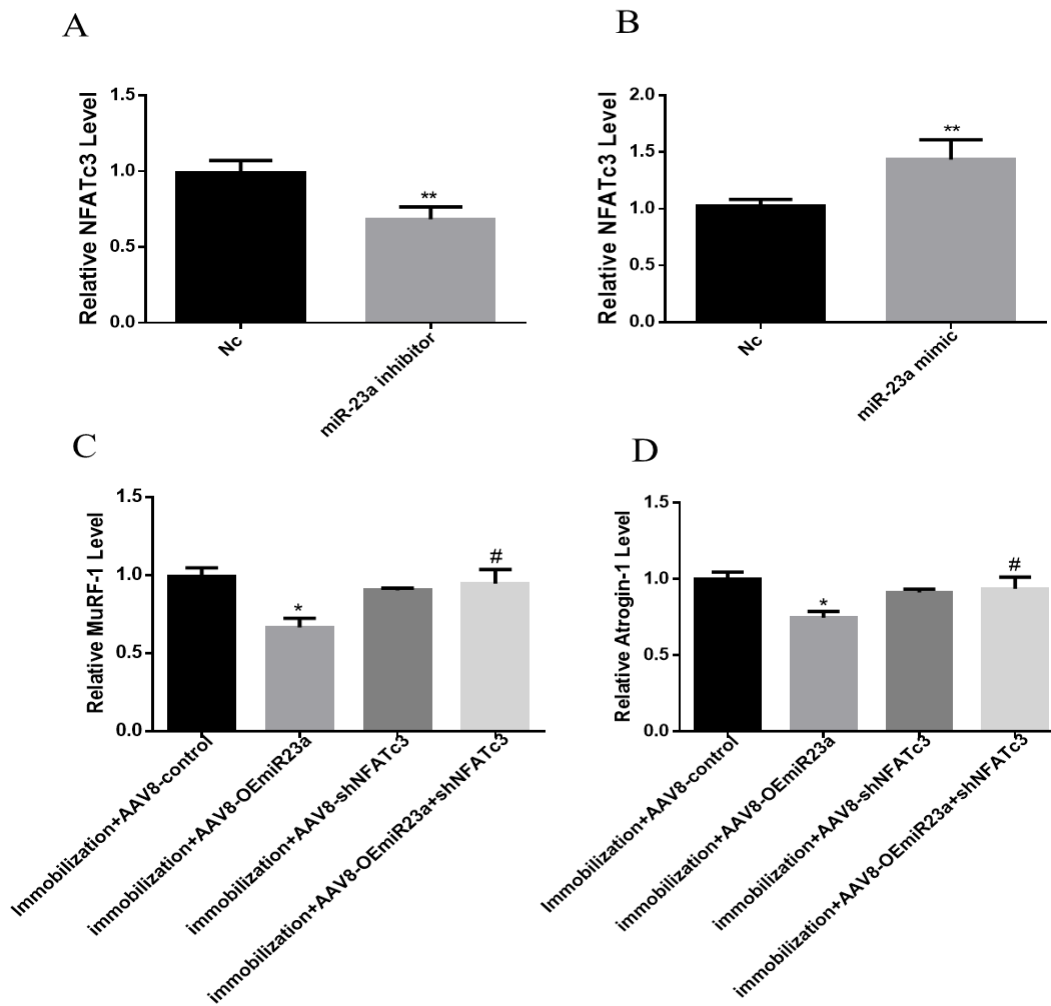


**Figure 3:** Interaction between miR-23a and NFATc3 Regulates Muscle Atrophy Process. A: Changes in NFATc3 expression in muscle tube cells of the miR-23a inhibitor group compared to the Nc group, \*\*,  $P < 0.01$ ,  $n = 6$ ; B: Changes in NFATc3 expression in muscle tube cells of the miR-23a mimic group compared to the Nc group, \*\*,  $P < 0.01$ ,  $n = 6$ ; C: Fluorescence quantitative PCR detection of MuRF-1 expression changes in the mouse gastrocnemius muscle, \*, #,  $P < 0.05$ ,  $n = 3$ ; D: Fluorescence quantitative PCR detection of Atrogin-1 expression changes in the mouse gastrocnemius muscle, \*, #,  $P < 0.05$ ,  $n = 3$ . \*: immobilization+AAV8-OEmiR23a vs immobilization+AAV8-control; #: immobilization+AAV8-OEmiR23a+ shNFATc3 vs immobilization+AAV8-OEmiR23a.

## Discussion

The mouse hindlimb immobilization model simulates muscle atrophy caused by disuse in humans very effectively. In previous studies, the soleus muscle of cast-immobilized mice decreased by 11% and 22% on days 3 and 7, respectively. In rat studies, the gastrocnemius muscle decreased by 12% after immobilization for 5 days (Miyachi *et al.*, 2023). Additionally, increased expression of MuRF1 and Atrogin-1 was observed in immobilized muscles. These results suggest that the immobilization model induces significant upregulation of E3 ubiquitin ligases MuRF1 and Atrogin-1, leading to muscle atrophy, which is consistent with our findings (Petrocelli *et al.*, 2024). Moreover, the hindlimb immobilization procedure does not require surgery or specialized equipment, and although surgically treated mice may suffer trauma during the procedure, it does not result in severe damage such as edema or necrosis. The ability to implant or remove both hindlimbs within 3 minutes allows researchers direct access to the immobilized muscles, facilitating the exploration of therapeutic drugs.

In recent years, there has been increasing interest in the functional roles of miRNAs in muscle atrophy. miR-24 promotes muscle cell development by inhibiting the cell cycle regulators Myc and E2F (Diniz & Wang, 2016; Drastichova *et al.*, 2023). miR-26 promotes muscle cell development by inhibiting histone methyltransferase Ezh2 (Murata *et al.*, 2017). miR-23a, a novel regulator of MuRF-1/Atrogin-1 gene transcription, plays an important role in preventing skeletal muscle atrophy. miR-23a has been reported to inhibit the occurrence of muscle atrophy caused by overload stress by specifically binding to the 3'UTR of muscle atrophy genes Atrogin-1 and MuRF-1, which is consistent with our results. We found that miR-23a expression was significantly decreased in the mouse hindlimb immobilization-induced muscle atrophy model, and the cross-sectional area of the muscles at the immobilized site decreased significantly after 7 days of hindlimb immobilization, accompanied by a significant increase in the expression of muscle atrophy markers Atrogin-1 and MuRF-1. We used AAV8 muscle local injection of miR-23a overexpression virus and found that overexpression of miR-23a could significantly alleviate muscle atrophy induced by hindlimb immobilization in mice, with a significant increase in muscle cross-sectional area. This lays a good foundation for the subsequent treatment of disuse muscle atrophy and can be used for the development of clinical therapeutic drugs.

Limitation of study: The study is conducted in a mouse model, which may not fully replicate the complexity of human muscle atrophy. Future studies should aim to validate these findings in human subjects or more clinically relevant models.

## Conclusion

Nuclear factor of activated T cells (NFAT) is a transcription factor with five subtypes. NFATc3 mediates calcineurin (Cn) proliferation (Yang *et al.*, 2022). NFATc3 is activated by Cn and increases miR-23a expression (Ran *et al.*, 2014). In our study, we found that inhibition of miR-23a expression in myoblasts differentiated into muscle tube cells resulted in downregulation of NFATc3 expression, while overexpression of miR-23a resulted in upregulation of NFATc3 expression. This indicates that there is a mutual regulatory effect between NFATc3 and miR-23a. However, simultaneous injection of AAV8-OEmiR-23a and AAV8-shNFATc3 into the gastrocnemius muscle did not alleviate the increased expression of muscle atrophy markers MuRF-1 and Atrogin-1 caused by hindlimb immobilization, indicating that miR-23a and NFATc3 jointly regulate the process of muscle atrophy. However, the specific mechanism by which miR-23a and NFATc3 regulate muscle atrophy requires further investigation.

## Acknowledgments

The authors express their gratitude to the fund project supported by China Hainan Provincial Natural Science Foundation, Hainan Medical University, China, the faculty of medical science and the management of Lincoln University College, Malaysia, for providing all the necessary support and facilities to complete the present study.

Fund Project: Supported by China Hainan Provincial Natural Science Foundation, Approval Number: 821QN256, Project Name: "Effects of miR-23a on Fixed Muscle Atrophy in the Hind Limbs of Mice and Preliminary Mechanism Exploration"

## References

- Altana, V., Geretto, M., & Pulliero, A. (2015). MicroRNAs and physical activity. *Microna*, 4(2), 74-85. <https://doi.org/10.2174/2211536604666150813152450>
- Diniz, G. P., & Wang, D. Z. (2016). Regulation of skeletal muscle by microRNAs. *Compr. Physiol*, 6(3), 1279-1294. <https://doi.org/10.1002/cphy.c150041>
- Dong, W., Chen, X., Wang, M., Zheng, Z., Zhang, X., Xiao, Q., & Peng, X. (2019). Mir-206 partially rescues myogenesis deficiency by inhibiting CUGBP1 accumulation in the cell models of myotonic dystrophy. *Neurological Research*, 41(1), 9-18. <https://doi.org/10.1080/01616412.2018.1493963>
- Drastichova, Z., Trubacova, R., & Novotny, J. (2023). Regulation of phosphosignaling pathways involved in transcription of cell cycle target genes by TRH receptor activation in GH1 cells. *Biomedicine & Pharmacotherapy*, 168, 115830. <https://doi.org/10.1016/j.biopha.2023.115830>
- Horak, M., Novak, J., & Bienertova-Vasku, J. (2016). Muscle-specific microRNAs in skeletal muscle development. *Developmental biology*, 410(1), 1-13. <https://doi.org/10.1016/j.ydbio.2015.12.013>
- Ikenaka, A., Kitagawa, Y., Yoshida, M., Lin, C. Y., Niwa, A., Nakahata, T., & Saito, M. K. (2023). SMN promotes mitochondrial metabolic maturation during myogenesis by regulating the MYOD-miRNA axis. *Life science alliance*, 6(3). <https://doi.org/10.26508/lsa.202201457>
- Ismaeel, A., Van Pelt, D. W., Hettinger, Z. R., Fu, X., Richards, C. I., Butterfield, T. A., ... & Dupont-Versteegden, E. E. (2023). Extracellular vesicle distribution and localization in skeletal muscle at rest and following disuse atrophy. *Skeletal Muscle*, 13(1), 1-16. <https://doi.org/10.1186/s13395-023-00315-1>
- Koutalianos, D., Koutsoulidou, A., Mastroiannopoulos, N. P., Furling, D., & Phylactou, L. A. (2015). MyoD transcription factor induces myogenesis by inhibiting Twist-1 through miR-206. *Journal of cell science*, 128(19), 3631-3645. <https://doi.org/10.1242/jcs.172288>
- Kutz, L., Zhou, T., Chen, Q., & Zhu, H. (2022). A Surgical Approach to Hindlimb Suspension: A Mouse Model of Disuse-Induced Atrophy. In *Chemokine-Glycosaminoglycan Interactions: Methods and Protocols*. New York, NY: Springer US. 2597, 1-9. [https://doi.org/10.1007/978-1-0716-2835-5\\_1](https://doi.org/10.1007/978-1-0716-2835-5_1)
- Miyachi, R., Morita, Y., & Yamazaki, T. (2023). Division of loading time in reloading the disused atrophic soleus muscle induces proximal muscle injury. *Journal of Physical Therapy Science*, 35(3), 193-198. <https://doi.org/10.1589/jpts.35.193>
- Murata, M., Nonaka, H., Komatsu, S., Goto, M., Morozumi, M., Yamada, S., ... & Tachibana, H. (2017). Delphinidin prevents muscle atrophy and upregulates miR-23a expression. *Journal of agricultural and food chemistry*, 65(1), 45-50. <https://doi.org/10.1021/acs.jafc.6b03661>
- Petrocelli, J. J., Liu, J., Yee, E. M., Ferrara, P. J., Bourrant, P. E., de Hart, N. M., ... & Drummond, M. J. (2024). Skeletal muscle-specific inducible AMPK $\alpha$ 1/ $\alpha$ 2 knockout mice develop muscle weakness, glycogen depletion, and fibrosis that persists during disuse atrophy. *American Journal of Physiology-Endocrinology and Metabolism*, 326(1), E50-E60. <https://doi.org/10.1152/ajpendo.00261.2023>
- Ran, Y., Wu, H., Wei, L., Yu, X., Chen, J., Li, S., Zhang, L., Lou, J., & Zhu, D. (2014). NFATc3 pathway participates in the process that 15-LO/15-HETE protects pulmonary artery smooth muscle cells against apoptosis during hypoxia. *Journal of Receptors and Signal Transduction*, 34(4), 270-282. <https://doi.org/10.3109/10799893.2014.917322>
- Reidy, P. T., Smith, A. D., Jevnikar, B. E., Doctor, A. K., Williams, R. W., Kachulkin, A. A., ... & Drummond, M. J. (2023). Muscle disuse as hindlimb unloading in early postnatal mice negatively impacts grip strength in adult mice: a pilot study. *Journal of Applied Physiology*, 134(4), 787-798. <https://doi.org/10.1152/jappphysiol.00681.2022>
- Ryu, Y., Lee, D., Jung, S. H., Lee, K. J., Jin, H., Kim, S. J., ... & Won, K. J. (2019). Sabinene prevents skeletal muscle atrophy by inhibiting the MAPK-MuRF-1 pathway in rats. *International Journal of Molecular Sciences*, 20(19), 4955. <https://doi.org/10.3390/ijms20194955>
- Takahashi, I., Matsuzaki, T., Kuroki, H., & Hoso, M. (2023). Treadmill exercise suppresses histological progression of disuse atrophy in articular cartilage in rat knee joints during hindlimb suspension. *Cartilage*, 14(4), 482-491. <https://doi.org/10.1177/19476035231154510>
- Wang, H., Wang, H., Li, X., & Xu, W. (2024). MuRF-1 is Involved in Laryngeal Muscle Denervation Atrophy by Regulating G-Actin Ubiquitination. *The Laryngoscope*, 134(2), 855-864. <https://doi.org/10.1002/lary.31021>
- Yang, Y. S., Kim, J. M., Xie, J., Chaugule, S., Lin, C., Ma, H., ... & Shim, J. H. (2022). Suppression of heterotopic ossification in fibrodysplasia ossificans progressiva using AAV gene delivery. *Nature communications*, 13(1), 6175. <https://doi.org/10.1038/s41467-022-33956-9>